Water Resources Research

RESEARCH ARTICLE
10.1029/2019WR026192

Groundwater Buffers Drought Effects and Climate Variability in Urban Reserves

V. Marchionni[1], E. Daly[1], G. Manoli[2], N. J. Tapper[3], J. P. Walker[1], and S. Fatichi[4,5]

[1]Department of Civil Engineering, Monash University, Melbourne, Victoria, Australia, [2]Department of Civil, Environmental and Geomatic Engineering, University College London, London, UK, [3]School of Earth, Atmosphere, and Environment, Monash University, Melbourne, Victoria, Australia, [4]Institute of Environmental Engineering, ETH Zürich, Zürich, Switzerland, [5]Department of Civil and Environmental Engineering, National University of Singapore, Singapore

Key Points:
- Groundwater access is pivotal in supporting urban ecosystems functioning during prolonged droughts
- Soil water holding capacity strongly affects ecosystem response to groundwater depletion
- Groundwater access buffers the impacts of climate variability on ecosystem mass/energy fluxes

Correspondence to:
V. Marchionni,
valentinamarchionni@gmail.com

Citation:
Marchionni, V., Daly, E., Manoli, G., Tapper, N. J., Walker, J. P., & Fatichi, S. (2020). Groundwater buffers drought effects and climate variability in urban reserves. *Water Resources Research*, *56*, e2019WR026192. https://doi.org/10.1029/2019WR026192

Received 20 AUG 2019
Accepted 23 APR 2020
Accepted article online 27 APR 2020

Abstract Groundwater can have a critical role in sustaining the functioning of natural ecosystems during droughts, especially in dry and seasonally dry climates. However, the response to droughts of ecosystems embedded in urban areas is not well known. This study investigates how different scenarios of groundwater availability control the water balance and vegetation productivity of two urban reserves hosting native vegetation in the Melbourne metropolitan area, Australia. Using a mechanistic ecohydrological model supported by field observations, long-term simulations were run to explore the impact of groundwater flow on water, carbon, and energy fluxes under present climatic conditions, including the Millennium Drought (2001–2009), and in response to perturbations in key environmental variables (air temperature, atmospheric CO_2 concentrations, and rainfall). It was found that the presence of a water table and its capillary fringe within the root depths supports ecosystem transpiration and vegetation productivity. The effects of declining groundwater were found to be more severe in predominantly sandy soils because of the lower water holding capacity, identifying that the water status of vegetation differs significantly depending on soil type. Differences in rooting strategies and groundwater availability also had a pivotal role in helping plants soften the impacts of increased air temperature (T_a) and make use of higher atmospheric CO_2 concentrations. Increased T_a strongly affected evapotranspiration, enhancing the competition for water between different vegetation types. These results provide quantitative insights of how vegetation responds to groundwater depletion and climate variability, highlighting the essential role of groundwater resources in urban ecosystems characterized by seasonally dry climates.

1. Introduction

A considerable fraction of the global land area has the water table (WT) or its capillary fringe within the reach of plants roots (Fan et al., 2013). Therefore, groundwater is a key source of water for a wide range of terrestrial vegetation systems across different climatic regions, especially those characterized by pronounced dry seasons lasting for months (Fan, 2015; Lowry & Loheide, 2010). Consequently, groundwater could become increasingly important under a rapidly changing climate, as more frequent and severe extremes, such as droughts and hotter temperatures, increase the risk of plant mortality and reduce productivity (Allen et al., 2015; Breshears et al., 2005; Mcdowell et al., 2016; Qiu et al., 2019; Soylu et al., 2011). Groundwater depth has been found to control energy fluxes at the land surface, especially when the WT depth ranges between 1 and 5 m (Kollet & Maxwell, 2008; Maxwell & Kollet, 2008). In semiarid regions, for example, shallow WT near river corridors allows vegetation establishment and helps plants to cope with extended dry seasons (Scott et al., 2006). Other evidence of groundwater supporting plant water demand can be found in Mediterranean climates (Barbeta et al., 2015; Eamus et al., 2006; Murray et al., 2003; Zencich et al., 2002), where groundwater represents a large source of water for transpiration, possibly being the sole contribution to transpiration in parts of the year (Miller et al., 2010; Orellana et al., 2012). The contribution of the WT to forest transpiration has also been found in humid temperate climates (Love et al., 2018), even during cool and wet winter months (Vincke & Thiry, 2008).

The focus of most studies related to groundwater-dependent ecosystems is on large biodiverse ecosystems, often in natural environments or areas mildly affected by human activities. However, the role of groundwater in the water balance of urban ecosystems has received considerably less attention. In cities, vegetated surfaces become often fragmented into small and isolated patches of native species, which are surrounded

by impervious surfaces and embedded in a highly disturbed environment (McKinney, 2002). This complex mosaic of urban land use and cover strongly influences the water cycle (Bhaskar et al., 2016; Cho et al., 2009; Newcomer et al., 2014; Shields & Tague, 2015; Xiao et al., 2007), having impacts on rainfall partitioning into infiltration and runoff, plant available soil moisture, and, consequently, ecosystem health and productivity. Moreover, changes in air temperature associated with the urban heat island (UHI, Manoli et al., 2019) can increase the duration of the growing season of urban trees (Zipper et al., 2016), enhancing their transpiration rates when and where sufficient soil water is available to sustain the higher evapotranspirative demand (Zipper et al., 2017). In addition to these environmental changes, the need for fresh water in urban areas has exacerbated the pressure on groundwater resources, especially in fast-growing cities (Flörke et al., 2018). Because groundwater withdrawals and diversions may decrease groundwater levels, there is the need to evaluate if urban groundwater-dependent plants can be affected by more frequent, rapid, and extended WT declines and fluctuations than those in pristine environments (Naumburg et al., 2005).

While the role of urban trees in providing ecosystem services is well documented (Chiesura, 2004; Dobbs et al., 2014; Livesley et al., 2016; Song et al., 2018; Richards & Thompson, 2019; Tyrväinen et al., 2005), less is known about their response to environmental changes. In particular, groundwater-supported trees might cope with short-term droughts and hotter temperatures (Drake et al., 2018; Marchionni et al., 2019) better than with long-term groundwater storage declines due to climate shifts or direct anthropogenic manipulations (Eamus et al., 2015; Kløve et al., 2014). Investigating the interactions and feedback between WT dynamics and terrestrial vegetation becomes crucial for managing and maintaining healthy urban ecosystems and in gaining an understanding of possible impacts on land surface fluxes (Naumburg et al., 2005; Orellana et al., 2012).

This study has evaluated the vulnerability of urban vegetation to changes in environmental variables by using simulations of present conditions, tested against observations and a series of numerical experiments, for two urban reserves within the Melbourne metropolitan area in southeast Australia. Numerical simulations were carried out with a mechanistic ecohydrological model. The specific questions addressed are as follows: (1) How do different scenarios of groundwater availability control tree transpiration and vegetation productivity under both present and variable climate? (2) How can different vegetation types (tree-shrubs-grass) coexist, and is this coexistence threatened? (3) How can soil properties amplify or dampen the ecosystem dependence on groundwater?

2. Methods

The mechanistic ecohydrological model Tethys-Chloris (T&C) (Fatichi et al., 2014) was used to study two urban reserves hosting native vegetation within the Melbourne metropolitan area in southeast Australia. The recent Millennium Drought (Freund et al., 2017), a prolonged period of dry conditions spanning from 2001 to 2009, provided a unique opportunity to explore ecosystem response to changes in water availability. During this prolonged drought, below median rainfall (since at least 1900) was recorded along with regional declines in WT depths (Leblanc et al., 2012; van Dijk et al., 2013) and reductions of observed vegetation biomass (Sawada & Koike, 2016).

2.1. Sites and Data Description

Two small natural reserves located in the Melbourne metropolitan area in southeast Australia (Figure 1) were selected as case study: National Drive Reserve (38.03° S, 145.24° E; 14 m a.s.l.) and Alex Wilkie Reserve (37.58° S, 145.15° E; 27 m a.s.l.). The two reserves host predominantly native plants, with some introduced species, but differ in terms of vegetation structure and soil characteristics. Because a detailed description of the sites is already provided in Marchionni et al. (2019), only a brief summary is reported here.

National Drive is a 14 ha grassy woodland dominated by *Eucalyptus camaldulensis* with a stand density of about 500 trees per hectare and a mean diameter at breast height (DBH) of 293 mm; the soil across the site is predominantly clay. Alex Wilkie, located 10 km northwest of National Drive, is a 1.8 ha sandy plain woodland populated mostly with *Eucalyptus viminalis* and a dense understory of lower trees and shrubs (e.g., *Allocasuarina littoralis* and *Banksia marginata*) with a stand density of about 515 trees per hectare and a mean DBH of 203 mm. A shallow WT is within the reach of the plants root zone at both sites, potentially making vegetation dependent on groundwater.

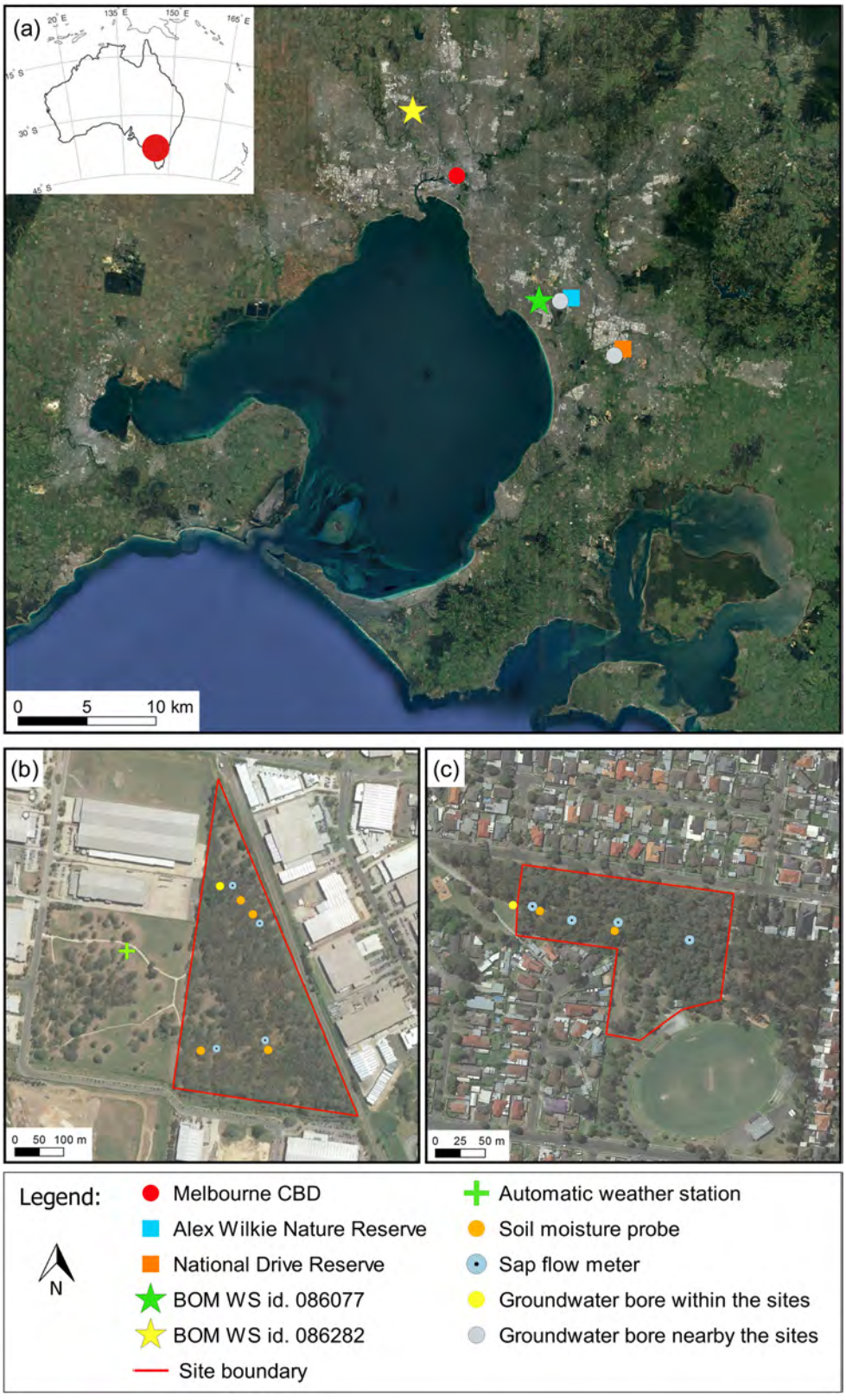

Figure 1. (a) Location map of the study sites, long-term groundwater wells, and Bureau of Meteorology weather stations (BOM WS) for Moorabbin Airport (No. 086077; 37.98° S, 145.24° E; elevation: 12 m) and Melbourne Airport (No. 086282; 37.67° S, 144.83° E; elevation: 113 m). Monitoring network at (b) National Drive Reserve and (c) Alex Wilkie Reserve.

Hydrological measurements were collected from December 2016 to June 2018 every 15 min at both sites, unless otherwise noted. Meteorological data, including rainfall, air temperature and relative humidity, wind speed, and incoming shortwave radiation were collected at National Drive using an automated weather station (Campbell Scientific). Long-term (July 1999 to June 2018) meteorological data were also available from the Bureau of Meteorology (BOM) weather stations network. Rainfall, air temperature and relative humidity, and wind speed at Moorabbin Airport (BOM Station No. 086077; 37.98° S, 145.24° E), and solar radiation at Melbourne Airport (BOM Station No. 086282; 37.67° S, 144.83° E) were additionally used to complete the meteorological forcing. Measurements of soil volumetric water content in the first 120 cm of the soil profile were taken at both sites (Drill & Drop by Sentek), with four profiles across National Drive and two at Alex Wilkie. WT depths were recorded from one bore at each site; atmospheric pressure was also measured in the bores. Sap flux density (SFD, $cm^3\ cm^{-2}\ hr^{-1}$) was measured at half-hourly intervals in four trees in each site using commercially available sap flow sensors (SFM1, ICT International, Australia) between February 2017 and April 2018. SFD measurements were scaled up to estimate the total transpiration for each reserve (Marchionni et al., 2019).

The climate of the area is Mediterranean (Cfa in the Köppen classification) with an average daily air temperature and annual rainfall of 15 ± 4.7° C and 639 ± 160 mm $year^{-1}$, respectively, for the period 1999–2018. The average reference potential evapotranspiration (ET_0) is about 1,286 mm $year^{-1}$ over the period 2010–2018 (https://www.bom.gov.au/watl/eto/), exceeding always rainfall (average P/ET_0 of 0.53). Long-term WT depth observations in eight wells were also available within 7 km radius from the study sites from 1 July 1999 to 30 June 2016 (https://www.vvg.org.au).

2.2. T&C Model

Model simulations were carried out using T&C (Fatichi et al., 2012, 2014; Manoli et al., 2018; Mastrotheodoros et al., 2019, 2020), which simulates essential components of the hydrological and carbon cycles, resolving energy, water, and carbon fluxes at the land surface. Meteorological inputs used for forcing T&C include rainfall, air temperature, relative humidity, wind speed, solar radiation, atmospheric pressure, cloud cover or longwave radiation, and atmospheric CO_2 concentration. Soil moisture dynamics are described by the one-dimensional (1-D) Richards equation for the vertical flow. T&C further accounts for biophysical and biochemical vegetation attributes using modules to simulate plant-related processes, such as photosynthesis, phenology, carbon pool dynamics, and tissue turnover (Fatichi & Pappas, 2017; Fatichi et al., 2014; Manoli et al., 2018). Vegetation species diversity can be explicitly represented at the species level, or more often by aggregating species that share the same life form and structural attributes, described as plant functional types (PFTs). In this study, two or three PFTs were used to account for the coexistence of trees, shrubs, and grass. The model can consider both horizontal and vertical composition of vegetation patches; in particular, the horizontal land cover composition accounts for the area occupied by each vegetation type. T&C simulates a number of ecohydrological variables including transpiration, soil evaporation, evaporation from interception, leakage at the soil bottom (or groundwater recharge), runoff, and profiles of soil moisture. It further simulates vegetation gross and net primary production, plant water stress, and leaf area index (LAI). Plant water stress is indicated with a factor, β, that expresses how the root integrated water potential departs from plant physiological thresholds characterizing incipient water stress. A reduction of β from 1 (unstressed conditions) affects plant photosynthesis and carbon allocation, and it can trigger leaf shedding.

2.3. Model Setup and Parameter Estimation

Consistent with the hypothesis of representing average reserve-scale processes, a 1-D soil domain was assumed with total soil depths limited to 15 and 7.2 m for a total of 41 and 36 vertical discretization layers at National Drive and Alex Wilkie, respectively. The soil vertical discretization is not uniform, with layer thickness becoming progressively thicker with depth, starting with the thinnest mesh stratum (0.01 m) at the surface. No-flow conditions were assigned at the bottom of the domain.

The modeled soil stratigraphy follows the one that was measured during the installation of the groundwater bores. In particular, at National Drive, the soil was assumed predominantly clay, whereas at Alex Wilkie, the soil was considered extremely sandy in the first 3.2 m, becoming more clayey with depth (Table 1). The specific soil hydraulic properties were obtained through pedotransfer functions (Saxton & Rawls, 2006) for National Drive, while the van Genuchten model (Carsel & Parrish, 1988; Van Genuchten, 1980) was used for Alex Wilkie, as the hydraulic parameters obtained by Saxton and Rawls (2006) pedotransfer functions led to

Table 1
Main Soil Parameters Used in the Simulations

Depth (m)	Soil discretization	Soil Sa/C/OM[a]	Van Genuchten coefficients (θ_s, θ_r, α, n)[b]	Saturated hydraulic conductivity (k_s; mm hr^{-1})[c]
National Drive				
0.0–0.3	Sandy loam	55/12/3	—	$k_s = -5.1, \ln(z) + 46.4$
0.3–0.6	Sandy clay loam	30/40/4	—	
0.6–1.2	Clay	8/80/1	—	
1.2–15	Clay	10/80/0.1	—	
Alex Wilkie				
0.0–3.2	Loamy sand	—	0.39, 0.025, 0.014 mm^{-1}, 1.95	$k_s = -39.6, \ln(z) + 339.3$
3.2–4.0	Silty loam	—	0.40, 0.070, 0.010 mm^{-1}, 1.60	
4.0–7.2	Silty clay	—	0.40, 0.120, 0.005 mm^{-1}, 1.10	

[a]Sa = sand; C = clay; OM = organic matter. Textural values are used as input to pedotransfer functions by Saxton and Rawls (2006). [b]Carsel and Parrish (1988). [c] k_s is assumed to be decreasing with depth (z; positive downward) according to a logarithmic law, which was derived starting from the values of k_s obtained in the calibration for the various soil texture classes, that is, 38 (sandy loam), 10 (sandy clay loam), 0.86 (clay), and 0.67 (clay) mm hr^{-1} for National Drive and 250 (loamy sand), 4 (silty loam), and 1 (silty clay) mm hr^{-1} for Alex Wilkie.

unrealistic soil moisture dynamics in such a soil with very high sand content. In both cases, soil hydraulic parameters were manually adjusted during calibration, as discussed in section 3.1.

Vegetation parameters (Table 2) were chosen based on literature and previous model application (Fatichi & Pappas, 2017). In particular, two PFTs (i.e., trees and grass) were considered at National Drive covering 40% and 60% of the reserve, respectively; at Alex Wilkie, the coexistence of trees, shrubs, and grass was

Table 2
Main Vegetation Parameters Used in the Simulations

		National Drive		Alex Wilkie		
Parameters	Unit	Trees	Grass	Trees	Shrubs	Grass
$Z_{R,50}$	m	0.35	0.15	0.60	0.50	0.20
$Z_{R,95}$	m	1.00	0.20	2.00	1.50	0.40
$ZR_{\max}$	m	3.00	0.30	4.00	3.80	0.50
h_c	m	20.00	0.20	20.00	10.00	0.20
a_1	—	8.00	7.00	8.00	6.00	7.00
ψ_{S2}	MPa	−0.70	−0.60	−0.70	−0.50	−0.60
ψ_{S50}	MPa	−1.50	−2.00	−1.50	−5.00	−2.00
S_L	m^2 gC^{-1}	0.009	0.016	0.009	0.012	0.016
r	gC gN^{-1} day^{-1}	0.042	0.038	0.042	0.036	0.038
$A_{L,cr}$	day	365	180	365	730	180
d_{mg}	day	20	20	20	15	20
T_{rr}	gC m^{-2} day^{-1}	1.00	2.50	1.00	0.40	2.50
L_{tr}	—	0.80	0.40	0.80	0.50	0.40
ϵ_{ac}	—	0.60	0.50	0.60	0.80	0.50
$1/K_{lf}$	day	40	40	40	50	40
$V_{c,\max 25}$	—	45	54	45	62	54
r_{JV}	—	2.00	2.10	2.00	2.00	2.10

Note. $Z_{R,50}$ = root depth 50th percentile; $Z_{R,95}$ = root depth 95th percentile; $Z_{R,\max}$ = maximum root depth; h_c = canopy height; a_1 = empirical parameter connecting stomatal aperture and net assimilation; ψ_{S2} = water potential at 2% stomatal closure; ψ_{S50} = water potential at 50% stomatal closure; S_L = specific leaf area; r = respiration rate at 10° C; $A_{L,cr}$ = critical leaf age; d_{mg} = days of maximum growth; T_{rr} = translocation rate from carbohydrate reserve; L_{tr} = leaf to root biomass maximum ratio; ϵ_{ac} = parameter for allocation to carbon reserves; $1/K_{lf}$ = dead leaf fall turnover; $V_{c,\max 25}$ = maximum Rubisco capacity at 25° C leaf level; r_{JV} = scaling $J_{\max}/V_{c,\max}$.

represented with three PFTs covering 20%, 20%, and 60% of the reserve, respectively. These fractions were based on local observations. A linear dose–response profile with tap roots (Collins & Bras, 2007) was used to describe the root depth distribution. This required specification of the rooting depth that contains 50% and 95% of fine root biomass ($Z_{R,50}$ and $Z_{R,95}$), as well as the maximum rooting depth ($Z_{R,\max}$).

The model was calibrated at hourly time steps to mainly reproduce soil water dynamics using the data collected between December 2016 and June 2018. Model performance in reproducing tree transpiration fluxes was also tested during this 19 month period. The atmospheric forcing consisted of meteorological data observed locally for National Drive and at the Moorabbin and Melbourne Airport weather stations for Alex Wilkie (Nos. 086077 and 086282). Soil moisture and vegetation carbon pool initial conditions for the calibration simulations were generated by running a 1 year spin-up simulation starting from soil moisture conditions coinciding with field capacity.

To account for local groundwater flow toward or from the sites, a net lateral flow (q) was added to the soil water budget. The amount of subsurface water entering and exiting the system was calculated using a simulation with q set to zero and impermeable soil bottom, meaning that the system is 1-D with no lateral flux of water; in such a case, plants can only use water stored in the root zone coming from rainfall. The term q was then obtained by matching the volume of water that the system needed in order to maintain the WT at the observed depth with fluctuations close to the ones measured. This approach allowed the estimation of the local net contribution of groundwater flow to the reserves. A 2-D or 3-D groundwater model would introduce many more uncertainties because of the lack of data to characterize the soil properties across the entire region (as the entire regional aquifer would need to be simulated) as well as a dearth of data on WT levels across the Melbourne metropolitan area. The values of q obtained during calibration are reported and discussed in section 3.1.

The values of the parameters obtained in the model calibration for National Drive and Alex Wilkie, including q, were then used to run long-term (July 1999 to June 2018) simulations to confirm the model performance in reproducing groundwater dynamics. For both sites, the long-term time series of meteorological data at the nearby Moorabbin Airport weather station was used. Results in terms of WT depths were then compared with the long-term observations available from the groundwater bores nearby the sites. Anomalies with respect to the mean value were evaluated to minimize the influence of topographic differences and spatial variability in the characteristics of the aquifers.

2.4. Numerical Experiments Under Present and Variable Climate

A series of numerical experiments were designed to investigate the effects of changes in soil water availability (both in the unsaturated and saturated zones) on hydrological fluxes and vegetation productivity. Simulations were carried out from 1 July 1999 to 30 June 2018 using the long-term time series of meteorological data available at the Moorabbin Airport weather station.

The sensitivity to groundwater availability was determined by imposing different values of q, leading to different WT depths: 0, 42, 63, 126, 252, and 378 mm year^{-1} for National Drive and 0, 50, 100, 200, 300, and 400 mm year^{-1} for Alex Wilkie. These scenarios were performed by assigning no-flow conditions at the bottom of the soil domain. A further scenario with free-drainage conditions and $q = 0$ mm year^{-1} (indicated as 0_{FD}) was also considered, for a total of seven scenarios in each site. Moreover, the impacts of the Millennium Drought on vegetation dynamics were analyzed by running a scenario with a lower q during the drought, thus taking into account a possible reduction of local groundwater flow toward the sites. Specifically, values of q equal to 63 and 100 mm year^{-1} were assumed between 2001 and 2009 (representing half of the estimated net groundwater flow) for National Drive and Alex Wilkie, respectively, while for the remaining years, q was set equal to 126 mm year^{-1} for National Drive and 200 mm year^{-1} for Alex Wilkie.

The effects of altered environmental drivers due to expected climate change were then investigated by imposing changes to air temperature, atmospheric CO_2 concentrations, and rainfall with respect to the present climate values. Simulations were run by changing only one environmental driver at a time to analyze their influence on vegetation response and hydrological fluxes. Specifically, four scenarios of increased temperature (+1.5° C, 2.0° C, 3.0° C, and 4.0° C), two scenarios with increased atmospheric CO_2 concentrations (+200 and +400 ppm), and two different rainfall conditions (+15% and −15%) were simulated. In all simulations, soil moisture and vegetation carbon pools were initialized by running a spin-up period of 19 years.

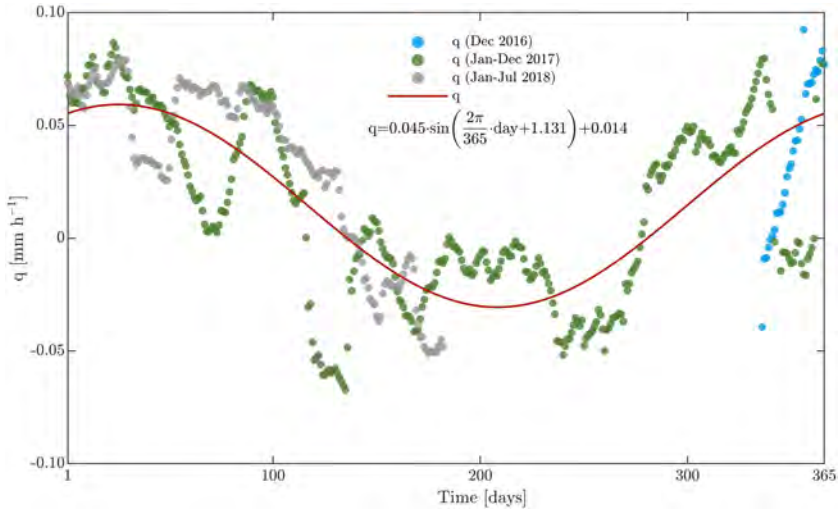

Figure 2. Net lateral flow (q) necessary to maintain the water table depth at the level of observations for the 19 month calibration period at National Drive Reserve. Values are shown for December 2016 (blue dots), January to December 2017 (green dots), and January to July 2018 (gray dots). A sinusoidal function (red line) was then fitted to smooth annual variation of q and its observational uncertainty.

3. Results

3.1. Model Calibration and Confirmation

A satisfactory match between observed and simulated soil water dynamics was achieved for the 19 month calibration period at both sites, after tuning soil hydraulic properties (Table 1) and root depths (Table 2), as well as quantifying the net lateral flow (q).

The soil hydraulic parameters were homogeneous in the vertical direction within each soil texture class, except for the hydraulic conductivity at saturation (k_s), which was assumed to decrease with depth (z, positive downward) according to a logarithmic law. At each site, a specific equation was derived by fitting a logarithmic function to the values of k_s for the various soil texture classes (Table 1).

In terms of net lateral flow, an average q equal to 126 and 200 mm year^{-1} was estimated to reproduce the magnitude and timing of the WT fluctuations at National Drive and Alex Wilkie, respectively. Specifically, at National Drive, the values of q (represented by the dots in Figure 2), which can be either a source or a sink term, showed a clear seasonal pattern dependent on regional groundwater fluxes that balance the seasonal cycle of the evapotranspiration fluxes (ET) and maintain the WT at the observed depth. This seasonal cycle can be described with a sinusoidal function. This is particularly relevant at National Drive, where the WT level did not experience strong seasonal fluctuations, thus requiring q to have a seasonal cycle to balance ET. On the contrary, because the WT presents a mild seasonal cycle at Alex Wilkie, seasonal variations of q did not appear to be prominent at this site, with ET driving the cycle of WT. For this reason, a constant positive value of q (source) was assumed throughout the year at Alex Wilkie, as its seasonality is hard to disentangle from WT observation. The smaller value of net lateral flux q found for National Drive is likely reflecting local conditions and the local dynamics of the aquifer.

At National Drive, simulations exceeded the observed saturated zone during wet months, where the WT responded with a larger rise to less intense, more frequent rainfall events (Figure 3b). This was mainly due to the predominant clay soil that responds to small variations in volume of water with larger WT fluctuations. Overall, the model was able to reproduce the observed soil water dynamics in the unsaturated zone, that is, in the first 1.2 m of soil (Figure 3e). In particular, the match was relatively good for the surface soil layers (0–30 cm; R^2 = 0.41 and RMSE = 0.049 m^3 m^{-3}), which were also more sensitive to rainfall. Conversely, at depths of 30–70 cm (R^2 = 0.11 and RMSE = 0.040 m^3 m^{-3}) and 70–120 cm (R^2 = 0.10, RMSE = 0.037 m^3 m^{-3}), the model was not able to simulate the rapid increase in the water content, probably due to spatial variability of the soil properties that was not captured in this study, as well as the proximity to the WT. However, the RMSE values for all the soil layers were within (or slightly higher than) the range

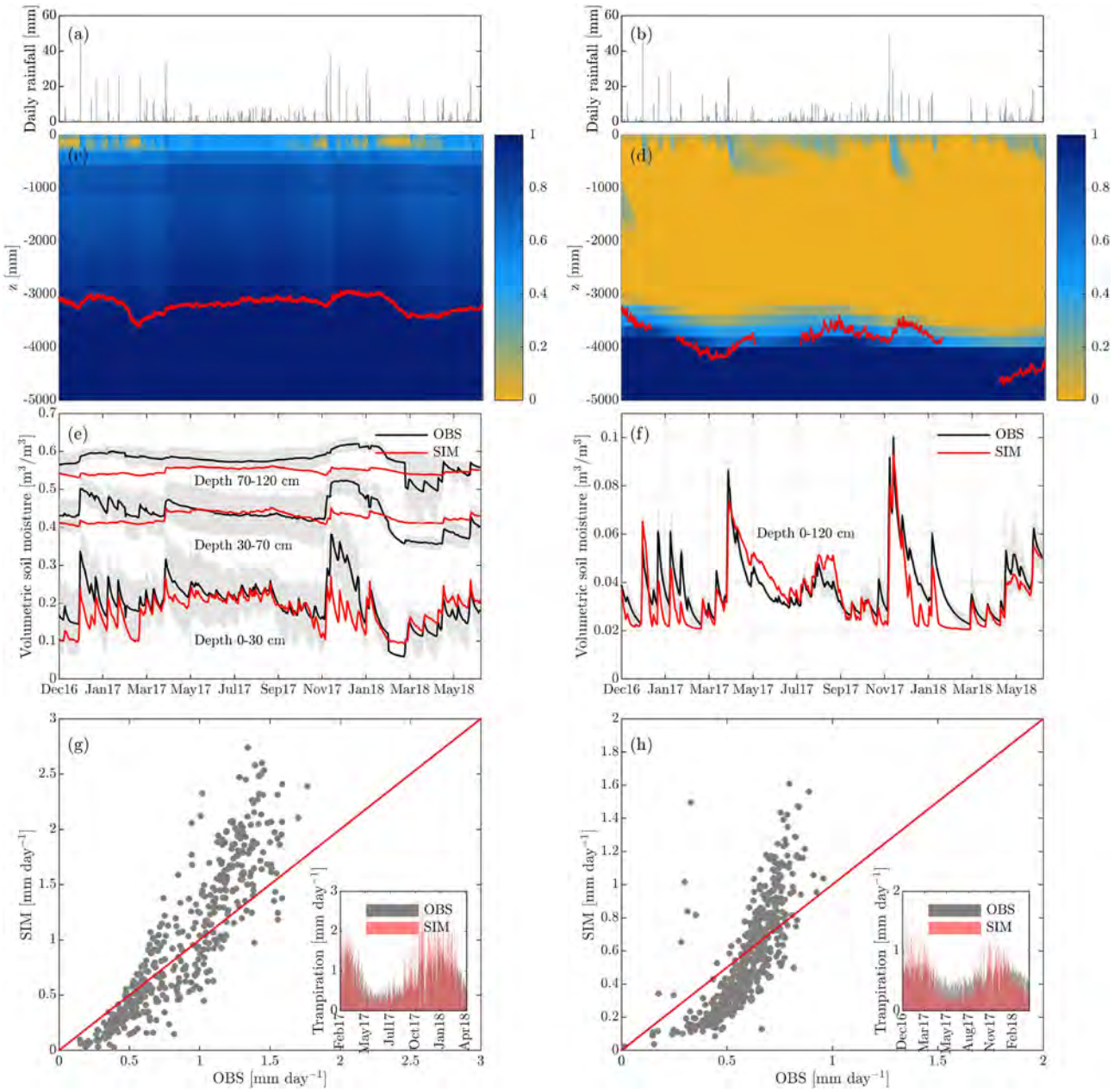

Figure 3. Daily rainfall recorded for the 19 month period between December 2016 and July 2018 at the (a) weather station located in National Drive Reserve and (b) Moorabbin Airport weather station for Alex Wilkie Reserve. A comparison between simulated effective saturation (S_e) and observed groundwater depths (red line) in the calibration period for (c) National Drive Reserve and (d) Alex Wilkie Reserve is presented. Simulated and observed (±SD; gray areas) volumetric soil moisture in the calibration period for (e) National Drive (at depths of 0–30, 30–70, and 70–120 cm) and (f) Alex Wilkie (depth of 0–120 cm) are also shown, along with simulated and observed transpiration (g) between February 2017 and April 2018 for National Drive and (h) between December 2016 and April 2018 for Alex Wilkie.

of 0.04 $m^3\ m^{-3}$ that often represents observation uncertainty, and it is considered acceptable for soil moisture modeling (Entekhabi et al., 2014). At Alex Wilkie, soil water dynamics in the top soil layers (Figure 3f) were generally well captured by the model ($R^2 = 0.70$, RMSE = 0.008 $m^3\ m^{-3}$), although they appeared to be disconnected from the saturated zone dynamics (Figure 3d). This was probably due to k_s decreasing with depth and preferential flows that were not accounted for in the model.

Although the model was not calibrated against transpiration rates, it was able to capture the dynamics of transpiration and its long-term value, with a slight overestimation of large rates and underestimation of low rates (Figures 3g and 3h). However, the errors in the measurements of sap flow, along with those occurring

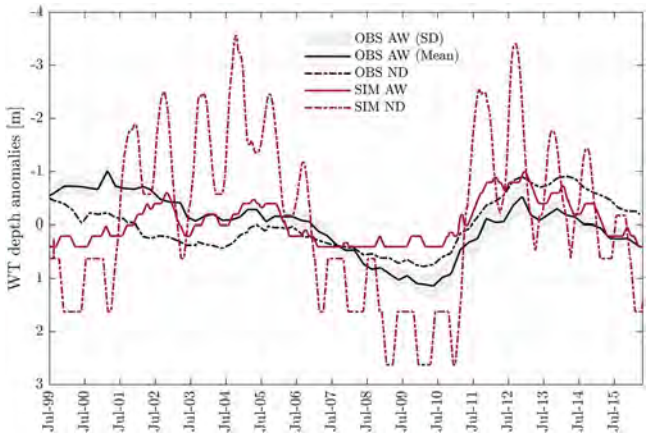

Figure 4. Simulated and observed water table (WT) fluctuations expressed as hourly anomalies (relative to the mean value) at both the observation bores within 7 km radius of and within the study sites.

during the upscaling as well as the strong variability in the measurements collected in the different trees at both sites suggest that the observed daily transpiration have large uncertainties.

A further confirmation of the model performance was achieved for the long-term (July 1999 to June 2016) WT fluctuations, expressed as hourly anomalies relative to the mean value (Figure 4). The model performed better at Alex Wilkie, whereas the amplitudes of the simulated anomalies were much more pronounced for National Drive, where the presence of the clay soil generated large changes in WT depths for small changes of water added or removed from the soil (e.g., a very small specific yield). In such a soil, it is observationally and numerically challenging to distinguish between actual WT depth and depth of the capillary fringe.

3.2. Ecohydrological Response to Soil Water Availability

The simulated effects of different groundwater levels on hydrological and energy fluxes as well as on plant water stress (β) and gross primary productivity (*GPP*) are shown in Figure 5, expressed as mean values of the 19 years analyzed, with *GPP* weighted and integrated over the entire vegetated area.

Groundwater availability, regulated by q, noticeably affected evapotranspiration fluxes (*ET*), which varied between 641 and 935 mm year^{-1} at National Drive (Figure 5a) and 640 and 985 mm year^{-1} at Alex Wilkie (Figure 5b) across the different simulation scenarios. The groundwater contribution led *ET* to exceed the mean annual precipitation, that is, 640 mm year^{-1}. In both reserves, results showed that an annual net lateral flow of 126 mm year^{-1} for National Drive and 200 mm year^{-1} for Alex Wilkie was sufficient to largely eliminate tree water stress. The WT depths obtained with these values of q (i.e., 6.9 m at National Drive and 3.9 m at Alex Wilkie) were considered the reference conditions for each site. At National Drive, grass transpiration (T_G) followed the same pattern as total *ET*, while tree transpiration (T_T) reached a maximum for q = 126 mm year^{-1} and then decreased slightly, as the WT was closer to the top soil layers and favors grass and ground evaporation. At Alex Wilkie, the presence of shrubs led to more complex dynamics associated with the competition for soil water resources, with T_G always below the shrubs transpiration (T_S) despite both having 20% of the areal cover. When the WT was 0.6 m below the ground, T_G reached its maximum (374 mm year^{-1}; +62%). T_T and T_S also increased considerably (+110% and +71%, respectively) when compared to the scenario 0_{FD} corresponding to a completely unsaturated soil column.

When groundwater was shallower than the reference value, a distinct increase in ground evaporation (*EG*) was modeled at National Drive because of the wet soil near the surface. This did not occur at Alex Wilkie as the sandy soil had little capillary rise, such that the WT had little to no effect on the moisture near the surface, thus resulting in low *EG*. Evaporation from interception, including interception in grass (EIn_G), trees (EIn_T), and shrubs (EIn_S) was a relatively minor component of the water balance at both sites, accounting for about 10% and 15% of the total *ET* at National Drive and Alex Wilkie, respectively. Overland runoff (*R*) was also quite small at both sites with it being mostly affected by low soil hydraulic conductivity of the superficial soil. The thicker capillary fringe due to the heavy clay soil of National Drive affected *R* even when the long-term average WT was below 3 m (going from 0 to 80 mm year^{-1} when the WT depth changed from 6.9 to 2.7 m), while at Alex Wilkie, the WT had to be on average only 0.6 m below the ground to generate runoff.

Changes in *ET* also affected the surface energy budget. Increasing groundwater availability led to higher latent heat (*LE*) and lower sensible heat (*H*) fluxes, resulting in a considerably different partitioning of energy at the land surface (i.e., lower Bowen ratio, $Bo = H/LE$) (Figures 5c and 5d).

In terms of plant water stress, results suggested that trees are more susceptible to water stress when deep roots do not have access to groundwater or its capillary fringe. In particular, at Alex Wilkie (Figure 5f), β for trees (β_T) strongly decreased (from 1 to 0.87) when the WT depth went below the reference value; on the contrary, at National Drive (Figure 5e), β_T remained overall above 0.97, due to the enhanced water holding capacity of the clay soil, which buffered the decline of WT. At both sites, grass was stressed in specific periods in all scenarios. While at National Drive, β for grass (β_G) increased from 0.90 to 0.94 when groundwater availability increased; at Alex Wilkie, it reached a maximum value (0.99) when the WT was on average

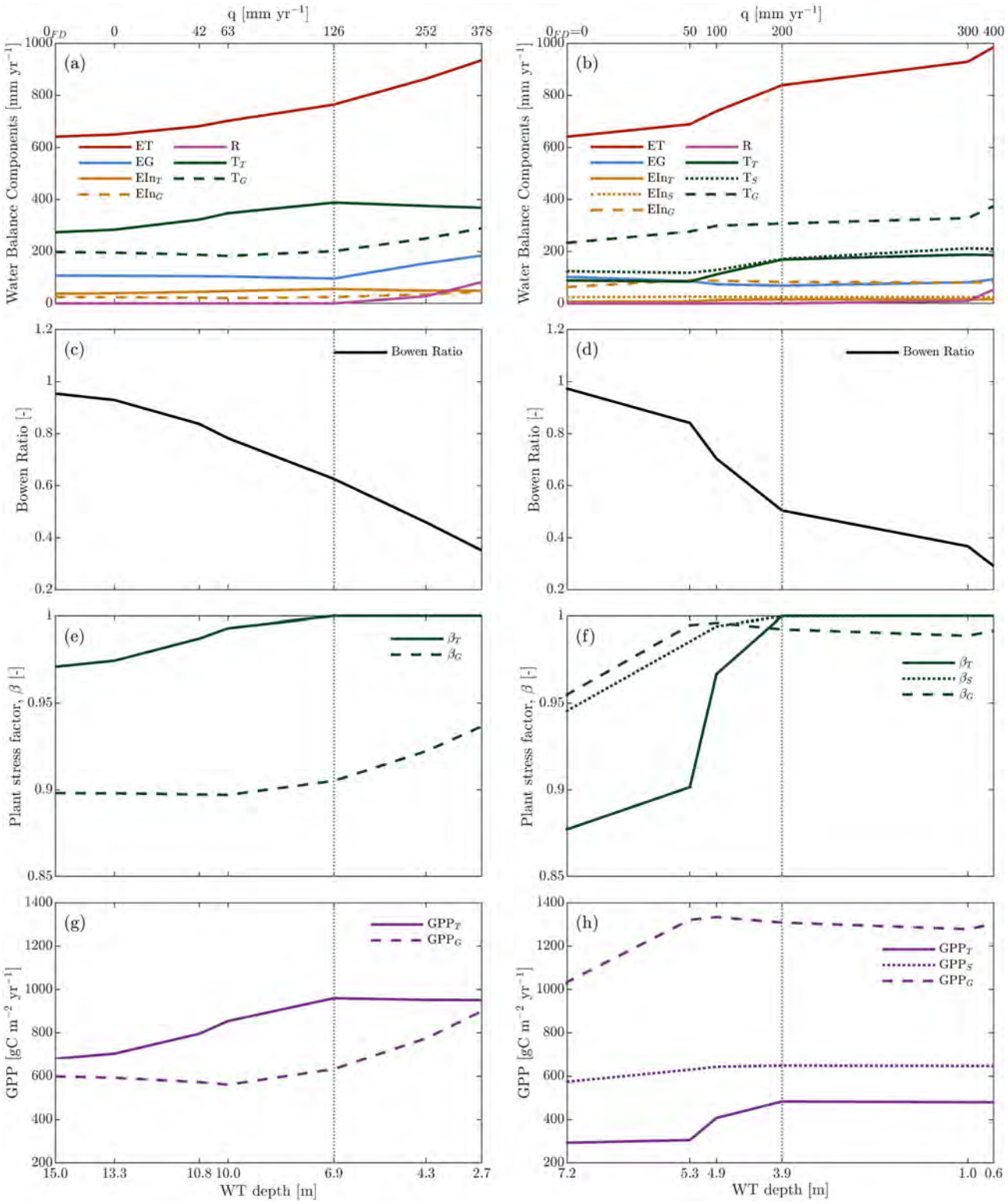

Figure 5. Simulation results averaged over the 19 year period (July 1999 to June 2018) illustrating water and energy fluxes as well as vegetation productivity with respect to different average water table (WT) depth scenarios (corresponding to different values of net lateral flow, q) at National Drive Reserve (left column) and Alex Wilkie Reserve (right column). (a, b) Water balance components (i.e., ET = evapotranspiration; EG = ground evaporation; EIn = evaporation from interception; R = runoff; T = transpiration; subscripts T, G, and S are referred to trees, grass, and shrubs, respectively), (c, d) Bowen ration ($Bo = H/LE$), (e, f) plant water stress (β), and (g, h) gross primary productivity (GPP; for unit of total ground area) are expressed as a function of both the average WT depth and average net lateral flow (q). The WT depth reference value, corresponding to the calibration period (dotted lines), is identified with q equal to 126 mm year^{-1} for National Drive Reserve and 200 mm year^{-1} for Alex Wilkie Reserve.

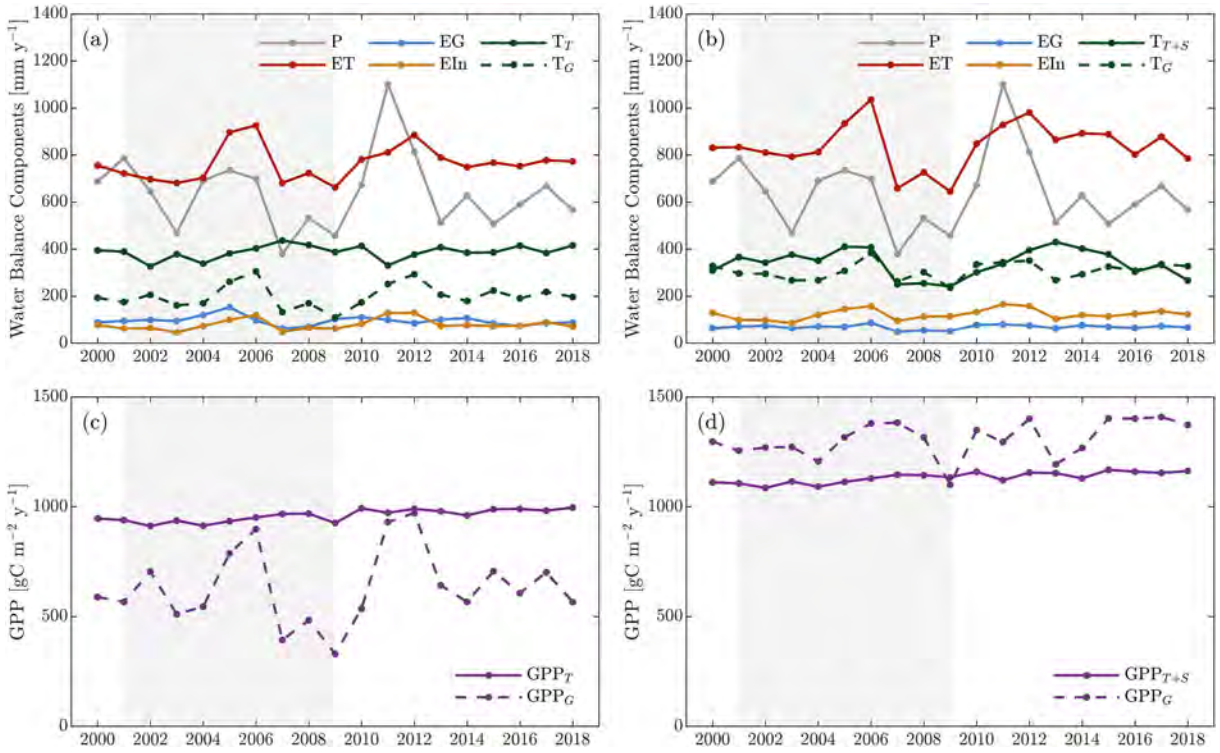

Figure 6. Simulation results for the 19 year period (July 1999 to June 2018) corresponding to the calibrated net lateral flow (q) of 126 mm year^{-1} for National Drive Reserve (left column) and 200 mm year^{-1} for Alex Wilkie Reserve (right column). (a, b) Annual values of the water balance components, that is, evaporation (*ET*), soil evaporation (*EG*), evaporation from interception summed over all PFTs (*EIn*), and transpiration from trees (T_T), grass (T_G), and trees and shrubs (T_{T+S}) combined. (c, d) Total annual values of gross primary productivity (*GPP*; for unit of total ground area) for trees (GPP_T), grass (GPP_S), and trees and shrubs (GPP_{T+S}) combined. Gray regions indicate the period of the Millennium Drought.

4.9 m below the ground, representing the best compromise in terms of competition with trees and shrubs. Shrubs at Alex Wilkie were less stressed than trees, with β for shrubs (β_S) always above 0.94 across the scenarios; this reflects a higher drought tolerance as specified in the model parameters, despite shallower roots than trees.

The impacts of groundwater availability were quite pronounced in terms of vegetation productivity. At both sites, the trajectories of gross primary productivity (*GPP*) with groundwater availability followed a similar trajectory as T_G, T_T, and T_S, with peaks in water use corresponding to peaks in productivity (Figures 5g and 5h). At National Drive, *GPP* of both grass (GPP_G) and trees (GPP_T) increased with groundwater availability (+41% and +50%, respectively). At Alex Wilkie (Figure 5h), GPP_T strongly decreased (−64%) when the average WT fell below 3.9 m, while *GPP* of shrubs (GPP_S) varied little with groundwater, remaining fairly constant across scenarios.

To explore the possible effects of the Millennium Drought (2001–2009) on the water fluxes and *GPP*, the time series of annual values of the main water fluxes and *GPP* were presented assuming the flux q to be as in the calibration period (Figure 6). At both sites, the simulated annual *ET* exceeded the annual precipitation (*P*) in most years. As the drought intensified between 2007 and 2009, grass cover at both sites appeared to be more stressed, leading to lower rates of transpiration and *GPP*; trees on the other hand, having access to groundwater, coped well with the drought, maintaining their unstressed transpiration rates and productivity. During the driest years of the Millennium Drought, that is, from 2007 to 2009, trees and shrubs reduced their transpiration at Alex Wilkie (Figure 6b), despite the constant net lateral flow of 200 mm year^{-1}.

When a decrease in local groundwater flow toward the sites was also taken into account during the prolonged drought (i.e., by reducing q by half), vegetation dynamics differed considerably compared to the scenario with constant q (Figure 7). In particular, trees appeared more stressed between 2007 and 2009 at Alex Wilkie, due to the dry conditions in the unsaturated zone and the very thin capillary fringe that could not buffer the groundwater drawdown. Simulations showed a rapid decrease in LAI_T (−26%) and GPP_T (−43%) between

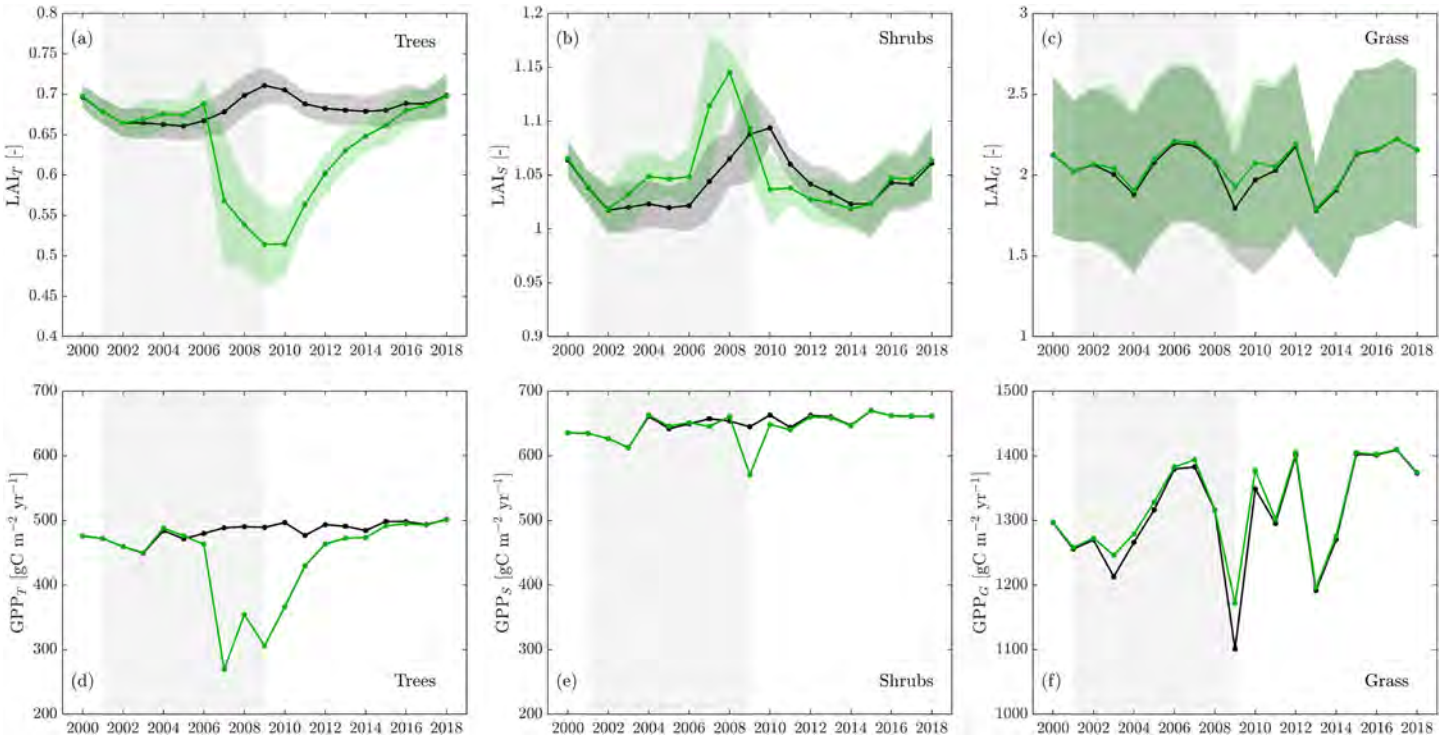

Figure 7. Simulation results for Alex Wilkie related to the 19 year period (July 1999 to June 2018) corresponding to a constant net lateral flow (q) of 200 mm year^{-1} (black lines) and a variable q (green lines), that is, 100 mm year^{-1} between 2001 and 2009 (Millennium Drought) and 200 mm year^{-1} in the remaining years. (a–c) Mean annual values (±SD) of leaf area index (*LAI*; for unit of total ground area) for (a) trees, (b) shrubs, and (c) grass. (d–f) Total annual values of gross primary productivity (*GPP*; per unit of total ground area) for (d) trees, (e) shrubs, and (f) grass. Gray regions indicate the period of the Millennium Drought.

2007 and 2009, followed by a slow recovery, returning in 2018 to the value that would have been obtained considering a constant q (Figures 7a and 7d). In contrast, groundwater drawdown did not have a strong impact on shrubs and grass dynamics due to the prolonged drought. Shrubs exhibited an increase in *LAI* between 2002 and 2008, due to the reduced competition with trees, followed by a steeper decrease compared to the constant q scenario (Figure 7b); in terms of *GPP*, simulations showed a slight decrease in GPP_S (−10%) in 2009 (Figure 7e). Both grass LAI_G and GPP_G (Figures 7c and 7f) were only slightly affected by the groundwater depletion, with an actual softening of water stress because of a minor competition with trees during the 2009–2011 period.

3.3. Sensitivity to Climate Variations

Simulations using different environmental drivers, that is, air temperature (T_a), atmospheric CO_2 concentrations, and rainfall (P), illustrate the possible role of groundwater in supporting these urban reserves to cope with plausible climatic variations. Results are shown with reference to two different groundwater availability scenarios: shallow groundwater (reference WT values, corresponding to the calibrated q) and without groundwater (completely unsaturated soil, corresponding to q sets to zero). Comparing these results with the simulation using observed climate, hereafter defined as control, groundwater availability strongly affects the water balance and vegetation productivity in both sites, even though soil properties and vegetation composition mediate the ecosystems response. Figures 8 and 9 show the results of the scenario analysis for National Drive and Alex Wilkie, respectively.

At National Drive, in shallow groundwater condition (Figure 8a), T_G and *EG* increased with T_a (22% and 43%, respectively), while T_T decreased (−17%). Without groundwater (Figure 8d), trees strongly reduced their transpiration (−31%) with increasing T_a, while T_G increased (31%) as a consequence of less competition; thus, in the simulation, grass was outcompeting trees in the access to the water in the top soil layers. Overall, T_a increases had a greater impact on plant water stress when deep roots did not have access to groundwater or its capillary fringe. While β_T decreased by 4% in the shallow groundwater scenario and by 8% in the scenario without groundwater (Figures 8b and 8e), β_G was not affected by groundwater presence, thus showing the

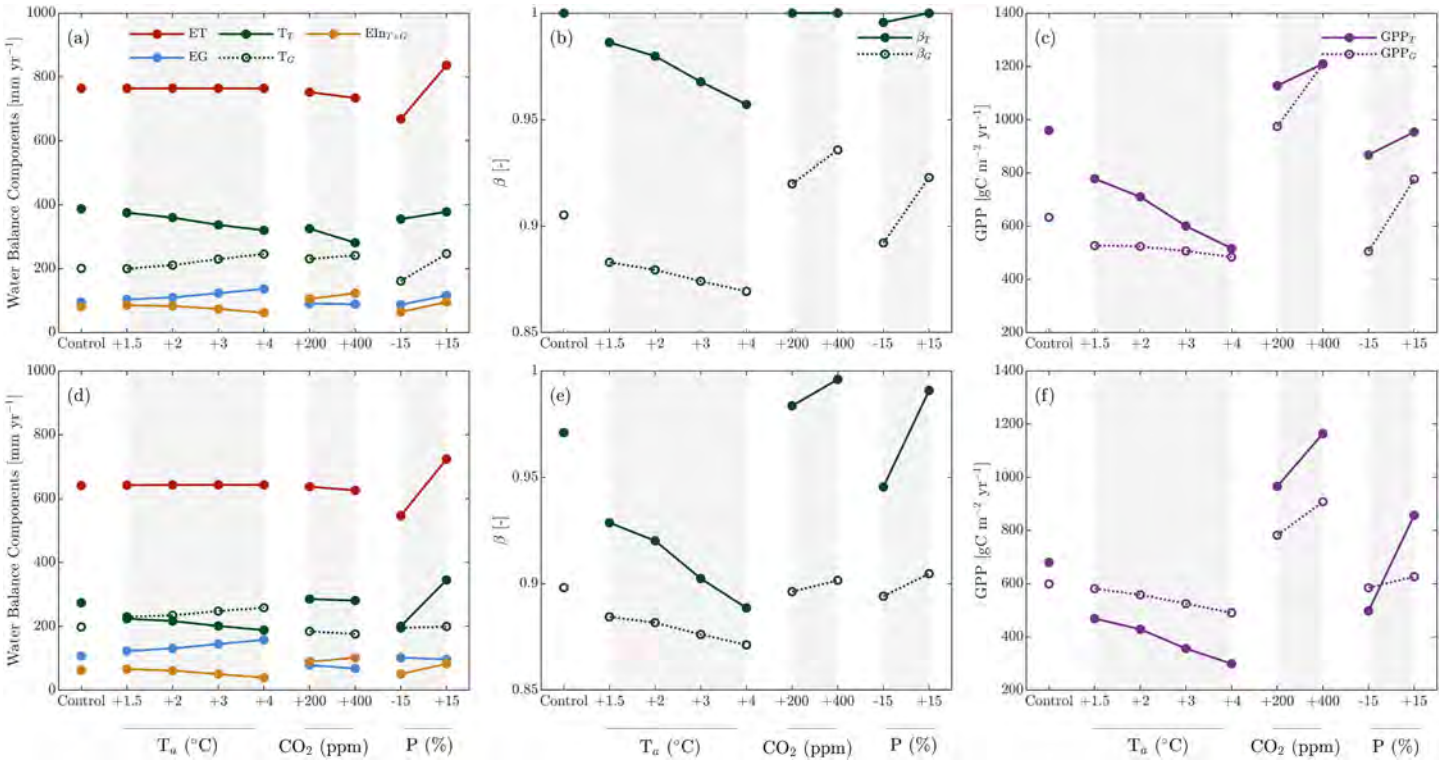

Figure 8. Effects of altered environmental drivers at National Drive for two different groundwater availability scenarios: (a–c) shallow groundwater (i.e., depth to groundwater at 6.9 m, corresponding to a net lateral flow of 126 mm year^{-1}) and (d–f) without groundwater (i.e., groundwater beneath the soil domain, corresponding to a net lateral flow of 0 mm year^{-1} and free drainage to the bottom of the soil domain). Simulation results show (a, d) water balance components (symbols as in Figure 5), (b, e) plant water stress (β), and (c, f) gross primary productivity (*GPP*; for unit of total ground area) for the actual climate and eight climate scenarios: four scenarios of increased air temperature T_a (+1.5° C, +2.0° C, +3.0° C, and +4.0° C), two scenarios with increased atmospheric CO_2 concentrations (+200 and +400 ppm), and two different rainfall (*P*) scenarios (+15% and −15%).

same decrease (3%) in both scenarios. Changes in water availability and air temperature were linked to changes in vegetation productivity, with GPP_T more affected than GPP_G. Results showed a steep decrease in GPP_T when T_a increased in both groundwater scenarios, decreasing by 56% with shallow WT (Figure 8c) and 18% with deep WT (Figure 8f). GPP_T overcame GPP_G when tree roots had access to groundwater, although in the +4° C scenario, the two values were similar; on the contrary, GPP_G overcame GPP_T across all temperature scenarios when groundwater was not accessible by tree roots.

In both scenarios, results indicated that with increased atmospheric CO_2, both grass and trees were able to assimilate carbon with a lower stomatal conductance and thus lower transpiration rate, leading to higher ecosystem water-use efficiency ($WUE = GPP/ET$). Specifically, by doubling the actual atmospheric CO_2 concentrations (+400 ppm), larger increases in *GPP* were found for the grass in the deep groundwater scenario (from 632 to 1,208 gC m^{-2} year^{-1}; +91%) and for the trees when groundwater was shallow (from 680 to over 1,164 gC m^{-2} year^{-1}; +71%). Overall, the increases in WUE were 59% and 74% in the shallow groundwater scenario and 71% and 67% in the scenario without groundwater, for grass and trees, respectively.

When they did not have access to groundwater, trees were more sensitive to rainfall variability, that is, a decrease in rainfall (−15%) led to −27% of T_T, while its increase (+15%) led to +26% of T_T; the same variations occurred in the GPP_T. Grass cover appeared to be more sensitive to rainfall variability for shallow WT depths. In particular, a decrease in rainfall (−15%) led to −20% of T_G and GPP_G, while its increase (+15%) generated a 23% increase of T_G and GPP_G.

Simulations in the shallow groundwater scenario at Alex Wilkie indicated that transpiration from trees and shrubs decreased when temperatures increased from the actual value (control simulation) to +4° C, leading to −52% for T_T and −40% for T_S; at the same time, grass transpiration increased (+24%) (Figure 9a). Without groundwater (Figure 9d), T_G remained fairly constant as the temperatures increased, while T_T and T_S exhibited a behavior consistent with the shallow groundwater scenario (−43% and −15%, respectively). Overall,

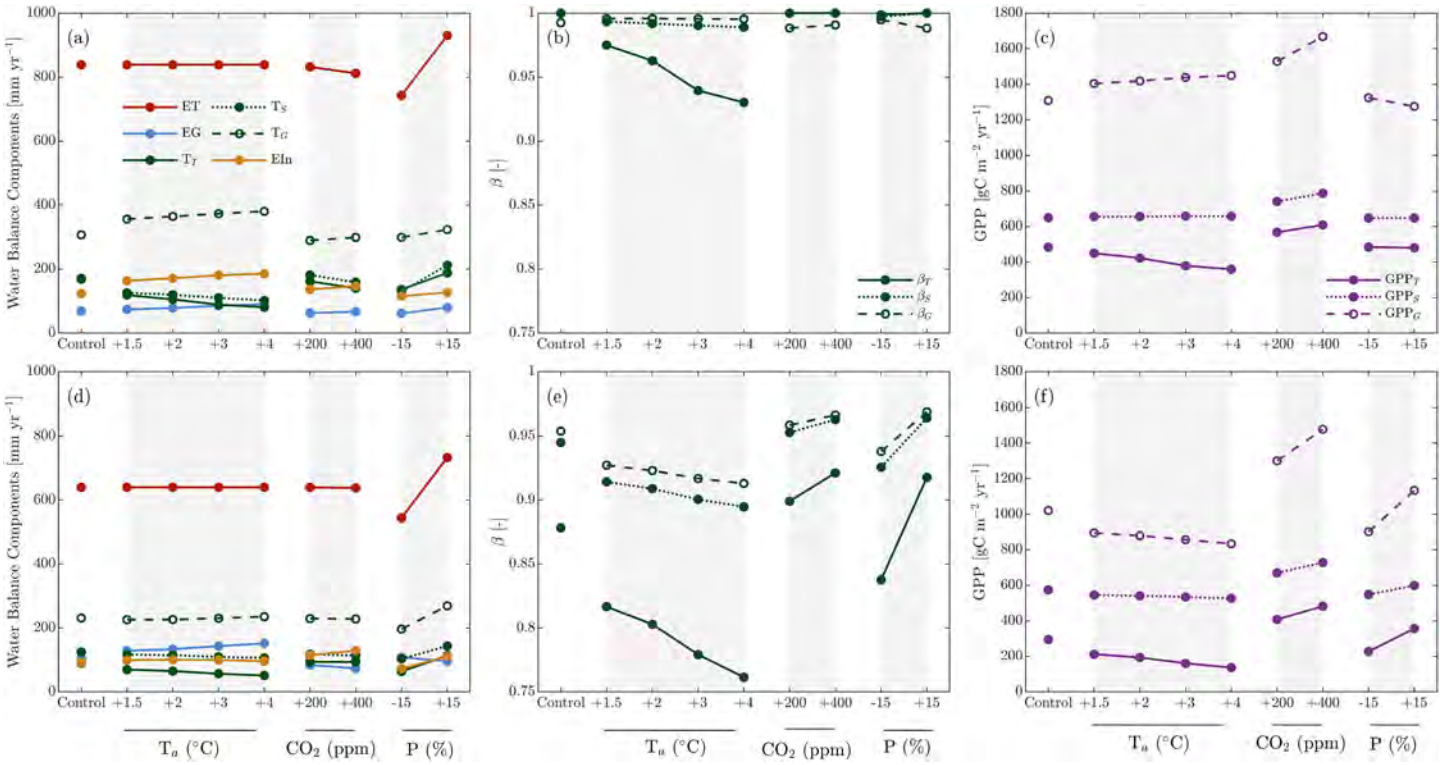

Figure 9. As for Figure 8 but for Alex Wilkie.

simulations indicated that grass and shrubs could cope quite well with T_a increases, in particular when the WT was within the reach of shrubs roots, with β_G remaining constant and β_S decreasing by 1%. Without the groundwater support, trees suffered most from the changes in T_a, with β_T decreasing by up to 13% (Figure 9b). In terms of vegetation productivity, trees were more susceptible to temperature increases than shrubs and grass, with GPP_T decreasing from 483 to 359 gC m^{-2} year^{-1} and from 295 to 137 gC m^{-2} year^{-1} for the shallow and no groundwater scenarios, respectively. Conversely, shrubs were affected very little by the changes in T_a, increasing by 1% when the WT was shallow and decreasing by 8% without groundwater (Figures 9c and 9f).

Similarly to National Drive, simulations for Alex Wilkie showed that changes in atmospheric CO_2 concentrations mainly influenced plant transpiration and productivity, increasing plant WUE. Higher increases in *GPP* were found for trees, shrubs, and grass in the deep groundwater scenario, that is, +63%, +27%, and +45%, respectively. Without groundwater, a decrease in rainfall considerably affected an already stressed ecosystem, leading to a reduction in T_T (−29%), T_S (−17%), and T_G (−15%). In contrast, a rainfall increase of 15% had a positive impact on trees, shrubs, and grass transpiration (+27%, +15%, and +16%, respectively).

4. Discussion

4.1. Dependence on Groundwater

The results of the numerical experiments showed how the presence of the WT or its capillary fringe within the root zone supported urban ecosystems against interannual rainfall variability. Groundwater availability was also found to have a pivotal role in helping plants soften the impacts of increased air temperature and profit from larger atmospheric CO_2 concentrations, as well as buffering the effects of local rainfall decrease. The presence of a shallow WT as well as the seasonal and interannual variations in WT depths arise from the variable balance between P, ET, and net lateral subsurface flow (q). Simulations showed that both National Drive and Alex Wilkie needed a considerable groundwater inflow at reserve scale to maintain the observed WT beneath the root zone, that is, 126 and 200 mm year^{-1} at National Drive and Alex Wilkie, respectively, which is roughly 20–30% of annual rainfall. These values of q led to a WT depth (expressed as mean value for the 19 year period of analysis) of 6.9 and 3.9 m for National Drive and Alex Wilkie, respectively, leading to an

increase in total *ET* of 19% and 31%, respectively. These levels of groundwater were sufficient to minimize the water stress and maximize plant productivity. Such result also highlighted the importance of including groundwater in ecohydrological analysis, given their essential role in controlling plant water stress in certain ecosystems (Brolsma & Bierkens, 2007; Brolsma et al., 2010).

Simulations indicated that woody plants overall transpired more (+42% at National Drive, i.e., 388 mm year^{-1}, and +90% at Alex Wilkie, i.e., 188 mm year^{-1}, Figure 5) in scenarios where the WT depth was maintained within the reach of the plant roots. This was experimentally confirmed at the two study sites, where shallow WT depths were found to support transpiration during dry months as well as hot days and nights (Marchionni et al., 2019). The fact that groundwater represents such a large source of the water needed for trees is consistent with the results from previous studies on groundwater-dependent vegetation. Using stable isotope analysis or water balance methods, it has been shown that the contribution of groundwater to the total transpiration in seasonally dry ecosystems can range from 15% up to 100% (Orellana et al., 2012). As groundwater approaches the soil surface, the strong capillary rise from the shallow WT also enhances the amount of water transpired by grasses (Soylu et al., 2011), as reflected in the model results here.

At National Drive, the high water holding capacity of clay soil played a crucial role in amplifying the capillary rise even with an average WT 2.7 m below the soil surface, thus increasing grass transpiration by 46%. At Alex Wilkie, where the soil is predominantly sandy and the capillary fringe is practically absent, the WT needed to be almost within the grass roots (<1 m) in order to enhance significantly grass transpiration. At both sites, the trajectories of *GPP* with groundwater availability followed patterns similar to transpiration for all the vegetation types. As the WT deepened, declines in *GPP* were predicted in trees, shrubs, and grass, with trees experiencing a more consistent increase in water stress and hence a reduction in *GPP* relative to grass (Koirala et al., 2017). In particular, tree productivity decreased by about 40% (National Drive) and 64% (Alex Wilkie) when the WT was assumed to be out of reach (absent) compared to the reference WT scenario.

4.2. Vegetation Competition

Results from this study indicate that the presence of groundwater strongly affects the competition for water between woody plants (i.e., trees and shrubs) and grasses. Differences in terms of rooting depth and tolerance to low water potentials are critical for plant water access, canopy transpiration, and carbon assimilation, thus allowing for coexistence of woody plants and grasses (Eggemeyer et al., 2009). Shallow-rooted grass species only access soil moisture in the shallow soil layers, while trees and shrubs have access to the water in both shallow and deep soil layers (Kim & Eltahir, 2004; Rossatto et al., 2012). When groundwater is available, these differences in rooting and water uptake depths help buffer the competition for water (Grossiord et al., 2018). When the WT depth falls below a certain threshold level, capillary rise from the WT becomes inadequate to supply moisture to the woody plants, affecting their productivity and competitive performance. This can be noticed especially at Alex Wilkie, where, in addition to the higher species competition (i.e., coexistence of trees, shrubs, and grass), the effects of declining groundwater were more severe due to the sandy soil and low water holding capacity. Therefore, trees were more stressed at Alex Wilkie compared to National Drive when the WT is beneath their root zone, suggesting that the water status and competitiveness of vegetation may differ significantly depending on soil type (Naumburg et al., 2005). Overall, grasses appeared less affected by groundwater fluctuations than woody plants in all scenarios, because grasses rely on rainfall rather than groundwater resources. Groundwater drawdown can benefit grasses because of a reduced competitive capability of the other vegetation types. Furthermore, unlike trees and shrubs, which try to maintain their leaf area when stressed strongly regulating stomata (McDowell et al., 2008), grasses wilted reducing their leaf area and became almost inactive during dry periods.

4.3. Millennium Drought

During the Millennium Drought between 2001 and 2009, grass was more tolerant to changes in soil water availability (Craine et al., 2013). Even in such a prolonged dry period, trees and shrubs reliance on groundwater was sufficient to largely support ecosystem productivity and transpiration to levels similar to normal years. When, in addition to the rainfall shortage, a possible reduction in the groundwater flow toward the sites and thus a decrease in the WT depth were imposed, trees started showing signs of stress, manifested by a reduction in *LAI*, especially as drought condition intensified between 2007 and 2009. The extremely

dry sandy soil at Alex Wilkie did not provide any buffer to the groundwater drawdown, a buffer that was instead simulated at National Drive. After the Millennium Drought, a higher than average rainfall in 2010 in many parts of southeast Australia helped trees to recover from the water stress (van Dijk et al., 2013). However, simulations showed a full tree recovery only 5–6 years later, suggesting that long-term impacts on vegetation due to groundwater depletion combined with drought conditions may be possible.

4.4. Changing Climate

Groundwater availability was also found to have remarkable implications for ecosystems under different climatic conditions. The focus here was to explore the role of groundwater in affecting ecosystem response to a single forcing, such as higher air temperatures, increased atmospheric CO_2 concentrations, and different rainfall regimes. When subjected to warmer air temperatures, both urban reserves exhibited altered hydrologic regimes, especially when groundwater was out of reach. Although an increase in air temperature did not affect total evapotranspiration, it strongly affected its partitioning, in particular at National Drive, triggering an active competition for water sources between vegetation types. In all simulations, grass appeared to be able to cope better with increased temperature and maintain its transpiration and productivity levels. Without groundwater, the root water uptake also changed, thus resulting in higher competition for shallow soil water, as also shown by Grossiord et al. (2018). In these scenarios, grass was able to cope with modified conditions better than trees, profiting from the fact that the trees were more stressed. Already stressed by the lack of groundwater sources, trees quickly worsened their water stress under the warming climate. This was more evident at Alex Wilkie, where the low soil water holding capacity did not help to buffer the decline in groundwater. Warmer temperatures also contribute to lower photosynthesis rates (*GPP*), confirming that a warming climate combined with limited water availability reduces vegetation productivity (Grossiord et al., 2017; Raupach et al., 2013). In response to increased atmospheric CO_2, plants were able to photosynthesize with a lower stomatal conductance and thus with lower transpiration rates, leading to increased WUE, as expected (Frank et al., 2015; Keenan et al., 2013; Mastrotheodoros et al., 2017), regardless of the groundwater availability. This finding confirms that the high CO_2 environment expected for the future may partially alleviate water stress through increased WUE (Conley et al., 2001; Swann et al., 2016). Changes in rainfall of $\pm$15% were effective in modifying total *ET*, transpiration, and consequently vegetation productivity at both sites when the groundwater was deep. At National Drive, even with shallow WT, grasses were profiting of the augmented water availability.

5. Conclusion

A mechanistic ecohydrological model was used to simulate different scenarios of groundwater availability in two urban reserves hosting native vegetation within the Melbourne metropolitan area, Australia. Results from the numerical simulations confirmed that these ecosystems are dependent on groundwater, with the water transpired by woody plants (trees and shrubs) when the WT level is maintained within the reach of the plant roots being more than 40% of the average annual transpiration of the scenarios without groundwater. The fact that groundwater represents such a large source of water for these ecosystems emphasizes their vulnerability to its depletion, which, under certain scenarios, could result in reductions of plants transpiration (−56%) and productivity (−45%) and, in extreme cases, in drought-induced mortality (Eamus et al., 2015). Therefore, to be effective, the management of urban ecosystems should also account for groundwater dynamics. The most significant impacts of declining groundwater occurred in predominantly sandy soils because of their lower water holding capacity compared to clay soils.

Changes in environmental variables, such as increased air temperature and atmospheric CO_2 concentrations as well as a rainfall reduction, were found to alter ecosystems hydrologic regime and the competition among vegetation types, especially when groundwater was not available. These findings suggest that groundwater has a pivotal role in sustaining the analyzed urban reserves and even more so during major droughts or changes in climate.

Human-induced land use changes combined to a rapidly changing climate might threaten groundwater availability, with possible profound impacts on the conservation of natural ecosystems embedded in urban areas. Hence, extensive groundwater monitoring networks and robust quantifications of vegetation responses to groundwater depletion and climate variability, as computed here by means of ecohydrologic simulations, are crucial to guide and evaluate appropriate management practices.

Acknowledgments
V. M., E. D., N. T., and J. P. W. acknowledge the support of the Australian Research Council and the City of Greater Dandenong and Mooney Valley City councils through the Linkage Project LP150100901. G. M. was supported by the "The Branco Weiss Fellowship—Society in Science" administered by ETH Zürich. Meteorological data reported in this paper are available at the Bureau of Meteorology (BOM) website (https://www.bom.gov.au/climate/data/) (Moorabbin Airport Weather Station No. 086077 and Melbourne Airport Weather Station No. 086282). Groundwater observations are available at the website (https://www.vvg.org.au) (Bore Nos. 125270-1a, 125270-1b, 125272-2a, 125272-2b, 127487-3, 125274-4, and 125269-5 for Alex Wilkie; Bore No. 62949-11a for National Drive). Monitoring data (i.e., meteorological data [only for National Drive], water table depth, volumetric soil moisture, and daily transpiration) recorded at the two study sites can be found at figshare repository (https://doi.org/10.26180/5e4d14aec32ce).

References

Allen, C. D., Breshears, D. D., & McDowell, N. G. (2015). On underestimation of global vulnerability to tree mortality and forest die-off from hotter drought in the Anthropocene. *Ecosphere*, *6*(8), 1–55.

Barbeta, A., Mejía-Chang, M., Ogaya, R., Voltas, J., Dawson, T. E., & Peñuelas, J. (2015). The combined effects of a long-term experimental drought and an extreme drought on the use of plant-water sources in a Mediterranean forest. *Global Change Biology*, *21*(3), 1213–1225.

Bhaskar, A. S., Jantz, C., Welty, C., Drzyzga, S. A., & Miller, A. J. (2016). Coupling of the water cycle with patterns of urban growth in the Baltimore metropolitan region, United States. *JAWRA Journal of the American Water Resources Association*, *52*(6), 1509–1523.

Breshears, D. D., Cobb, N. S., Rich, P. M., Price, K. P., Allen, C. D., Balice, R. G., et al. (2005). Regional vegetation die-off in response to global-change-type drought. *Proceedings of the National Academy of Sciences*, *102*(42), 15,144–15,148.

Brolsma, R., & Bierkens, M. (2007). Groundwater–soil water–vegetation dynamics in a temperate forest ecosystem along a slope. *Water Resources Research*, *43*, W01414. https://doi.org/10.1029/2005WR004696

Brolsma, V. R. J., Van Beek, L., & Bierkens, M. (2010). Vegetation competition model for water and light limitation. II: Spatial dynamics of groundwater and vegetation. *Ecological Modelling*, *221*(10), 1364–1377.

Carsel, R. F., & Parrish, R. S. (1988). Developing joint probability distributions of soil water retention characteristics. *Water Resources Research*, *24*(5), 755–769.

Chiesura, A. (2004). The role of urban parks for the sustainable city. *Landscape and Urban Planning*, *68*(1), 129–138.

Cho, J., Barone, V., & Mostaghimi, S. (2009). Simulation of land use impacts on groundwater levels and streamflow in a Virginia watershed. *Agricultural Water Management*, *96*(1), 1–11.

Collins, D., & Bras, R. (2007). Plant rooting strategies in water-limited ecosystems. *Water Resources Research*, *43*, W06407. https://doi.org/10.1029/2006WR005541

Conley, M. M., Kimball, B., Brooks, T., Pinter Jr, P., Hunsaker, D., Wall, G., et al. (2001). CO_2 enrichment increases water-use efficiency in sorghum. *New Phytologist*, *151*(2), 407–412.

Craine, J. M., Ocheltree, T. W., Nippert, J. B., Towne, E. G., Skibbe, A. M., Kembel, S. W., & Fargione, J. E. (2013). Global diversity of drought tolerance and grassland climate-change resilience. *Nature Climate Change*, *3*(1), 63.

Dobbs, C., Nitschke, C. R., & Kendal, D. (2014). Global drivers and tradeoffs of three urban vegetation ecosystem services. *PLoS One*, *9*(11), e113000.

Drake, J. E., Tjoelker, M. G., Vårhammar, A., Medlyn, B. E., Reich, P. B., Leigh, A., et al. (2018). Trees tolerate an extreme heatwave via sustained transpirational cooling and increased leaf thermal tolerance. *Global Change Biology*, *24*(6), 2390–2402.

Eamus, D., Hatton, T., Cook, P., & Colvin, C. (2006). *Ecohydrology: Vegetation function, water and resource management*: CSIRO Publishing.

Eamus, D., Zolfaghar, S., Villalobos-Vega, R., Cleverly, J., & Huete, A. (2015). Groundwater-dependent ecosystems: Recent insights from satellite and field-based studies. *Hydrology and Earth System Sciences*, *19*(10), 4229–4256.

Eggemeyer, K. D., Awada, T., Harvey, F. E., Wedin, D. A., Zhou, X., & Zanner, C. W. (2009). Seasonal changes in depth of water uptake for encroaching trees Juniperus virginiana and Pinus ponderosa and two dominant C_4 grasses in a semiarid grassland. *Tree Physiology*, *29*(2), 157–169.

Entekhabi, D., Yueh, S., O'Neill, P. E., Kellogg, K. H., Allen, A., Bindlish, R., et al. (2014). SMAP handbook–soil moisture active passive: Mapping soil moisture and freeze/thaw from space.

Fan, Y. (2015). Groundwater in the Earth's critical zone: Relevance to large-scale patterns and processes. *Water Resources Research*, *51*, 3052–3069. https://doi.org/10.1002/2015WR017037

Fan, Y., Li, H., & Miguez-Macho, G. (2013). Global patterns of groundwater table depth. *Science*, *339*(6122), 940–943.

Fatichi, S., Ivanov, V., & Caporali, E. (2012). A mechanistic ecohydrological model to investigate complex interactions in cold and warm water-controlled environments: 1. Theoretical framework and plot-scale analysis. *Journal of Advances in Modeling Earth Systems*, *4*, M05002. https://doi.org/10.1029/2011MS000086

Fatichi, S., & Pappas, C. (2017). Constrained variability of modeled *T*:*ET* ratio across biomes. *Geophysical Research Letters*, *44*, 6795–6803. https://doi.org/10.1002/2017GL074041

Fatichi, S., Zeeman, M. J., Fuhrer, J., & Burlando, P. (2014). Ecohydrological effects of management on subalpine grasslands: From local to catchment scale. *Water Resources Research*, *50*, 148–164. https://doi.org/10.1002/2013WR014535

Flörke, M., Schneider, C., & McDonald, R. I. (2018). Water competition between cities and agriculture driven by climate change and urban growth. *Nature Sustainability*, *1*(1), 51.

Frank, D., Poulter, B., Saurer, M., Esper, J., Huntingford, C., Helle, G., et al. (2015). Water-use efficiency and transpiration across European forests during the Anthropocene. *Nature Climate Change*, *5*(6), 579.

Freund, M., Henley, B. J., Karoly, D. J., Allen, K. J., & Baker, P. J. (2017). Multi-century cool-and warm-season rainfall reconstructions for Australia's major climatic regions. *Climate of the Past*, *13*(12), 1751–1770.

Grossiord, C., Sevanto, S., Bonal, D., Borrego, I., Dawson, T. E., Ryan, M., et al. (2018). Prolonged warming and drought modify belowground interactions for water among coexisting plants. *Tree Physiology*, *39*(1), 55–63.

Grossiord, C., Sevanto, S., Dawson, T. E., Adams, H. D., Collins, A. D., Dickman, L. T., et al. (2017). Warming combined with more extreme precipitation regimes modifies the water sources used by trees. *New Phytologist*, *213*(2), 584–596.

Keenan, T. F., Hollinger, D. Y., Bohrer, G., Dragoni, D., Munger, J. W., Schmid, H. P., & Richardson, A. D. (2013). Increase in forest water-use efficiency as atmospheric carbon dioxide concentrations rise. *Nature*, *499*(7458), 324.

Kim, Y., & Eltahir, E. A. (2004). Role of topography in facilitating coexistence of trees and grasses within savannas. *Water Resources Research*, *40*, W07505. https://doi.org/10.1029/2003WR002578

Kløve, B., Ala-Aho, P., Bertrand, G., Gurdak, J. J., Kupfersberger, H., Kværner, J., et al. (2014). Climate change impacts on groundwater and dependent ecosystems. *Journal of Hydrology*, *518*, 250–266.

Koirala, S., Jung, M., Reichstein, M., de Graaf, I. E., Camps-Valls, G., Ichii, K., et al. (2017). Global distribution of groundwater-vegetation spatial covariation. *Geophysical Research Letters*, *44*, 4134–4142. https://doi.org/10.1002/2017GL072885

Kollet, S. J., & Maxwell, R. M. (2008). Capturing the influence of groundwater dynamics on land surface processes using an integrated, distributed watershed model. *Water Resources Research*, *44*, W02402. https://doi.org/10.1029/2007WR006004

Leblanc, M., Tweed, S., Van Dijk, A., & Timbal, B. (2012). A review of historic and future hydrological changes in the Murray-Darling Basin. *Global and Planetary Change*, *80*, 226–246.

Livesley, S., McPherson, E., & Calfapietra, C. (2016). The urban forest and ecosystem services: Impacts on urban water, heat, and pollution cycles at the tree, street, and city scale. *Journal of Environmental Quality*, *45*(1), 119–124.

Love, D., Venturas, M., Sperry, J., Brooks, P., Pettit, J., Wang, Y., et al. (2018). Dependence of aspen stands on a subsurface water subsidy: Implications for climate change impacts. *Water Resources Research*, *55*, 1833–1848. https://doi.org/10.1029/2018WR023468

Lowry, C. S., & Loheide, S. P. (2010). Groundwater-dependent vegetation: Quantifying the groundwater subsidy. *Water Resources Research*, *46*, W06202. https://doi.org/10.1029/2009WR008874

Manoli, G., Fatichi, S., Schlpfer, M., Yu, K., Crowther, T. W., Meili, N., et al. (2019). Magnitude of urban heat islands largely explained by climate and population. *Nature*, *573*(7772), 55–60. https://doi.org/10.1038/s41586-019-1512-9

Manoli, G., Ivanov, V. Y., & Fatichi, S. (2018). Dry-season greening and water stress in Amazonia: The role of modeling leaf phenology. *Journal of Geophysical Research: Biogeosciences*, *123*, 1909–1926. https://doi.org/10.1029/2017JG004282

Manoli, G., Meijide, A., Huth, N., Knohl, A., Kosugi, Y., Burlando, P., et al. (2018). Ecohydrological changes after tropical forest conversion to oil palm. *Environmental Research Letters*, *13*(6), 64035.

Marchionni, V., Guyot, A., Tapper, N., Walker, J., & Daly, E. (2019). Water balance and tree water use dynamics in remnant urban reserves. *Journal of Hydrology*, *575*, 343–353.

Mastrotheodoros, T., Pappas, C., Molnar, P., Burlando, P., Hadjidoukas, P., & Fatichi, S. (2019). Ecohydrological dynamics in the Alps: Insights from a modelling analysis of the spatial variability. *Ecohydrology*, *12*(1), e2054.

Mastrotheodoros, T., Pappas, C., Molnar, P., Burlando, P., Keenan, T. F., Gentine, P., et al. (2017). Linking plant functional trait plasticity and the large increase in forest water use efficiency. *Journal of Geophysical Research: Biogeosciences*, *122*, 2393–2408. https://doi.org/10.1002/2017JG003890

Mastrotheodoros, T., Pappas, C., Molnar, P., Burlando, P., Manoli, G., Parajka, J., et al. (2020). More green and less blue water in the Alps during warmer summers. *Nature Climate Change*, *10*(2), 155–161. https://doi.org/10.1038/s41558-019-0676-5

Maxwell, R. M., & Kollet, S. J. (2008). Interdependence of groundwater dynamics and land-energy feedbacks under climate change. *Nature Geoscience*, *1*(10), 665.

McDowell, N., Pockman, W. T., Allen, C. D., Breshears, D. D., Cobb, N., Kolb, T., et al. (2008). Mechanisms of plant survival and mortality during drought: Why do some plants survive while others succumb to drought? *New phytologist*, *178*(4), 719–739.

McKinney, M. L. (2002). Urbanization, biodiversity, and conservation: The impacts of urbanization on native species are poorly studied, but educating a highly urbanized human population about these impacts can greatly improve species conservation in all ecosystems. *Bioscience*, *52*(10), 883–890.

Mcdowell, N. G., Williams, A., Xu, C., Pockman, W., Dickman, L., Sevanto, S., et al. (2016). Multi-scale predictions of massive conifer mortality due to chronic temperature rise. *Nature Climate Change*, *6*(3), 295.

Miller, G. R., Chen, X., Rubin, Y., Ma, S., & Baldocchi, D. D. (2010). Groundwater uptake by woody vegetation in a semiarid oak savanna. *Water Resources Research*, *46*, W10503. https://doi.org/10.1029/2009WR008902

Murray, B. B. R., Zeppel, M. J., Hose, G. C., & Eamus, D. (2003). Groundwater-dependent ecosystems in Australia: It's more than just water for rivers. *Ecological Management & Restoration*, *4*(2), 110–113.

Naumburg, E., Mata-Gonzalez, R., Hunter, R. G., Mclendon, T., & Martin, D. W. (2005). Phreatophytic vegetation and groundwater fluctuations: A review of current research and application of ecosystem response modeling with an emphasis on Great Basin vegetation. *Environmental Management*, *35*(6), 726–740.

Newcomer, M. E., Gurdak, J. J., Sklar, L. S., & Nanus, L. (2014). Urban recharge beneath low impact development and effects of climate variability and change. *Water Resources Research*, *50*, 1716–1734. https://doi.org/10.1002/2013WR014282

Orellana, F., Verma, P., Loheide, S. P., & Daly, E. (2012). Monitoring and modeling water-vegetation interactions in groundwater-dependent ecosystems. *Reviews of Geophysics*, *50*, RG3003. https://doi.org/10.1029/2011RG000383

Qiu, J., Zipper, S. C., Motew, M., Booth, E. G., Kucharik, C. J., & Loheide, S. P. (2019). Nonlinear groundwater influence on biophysical indicators of ecosystem services. *Nature Sustainability*, *2*(6), 475.

Raupach, M., Haverd, V., & Briggs, P. (2013). Sensitivities of the Australian terrestrial water and carbon balances to climate change and variability. *Agricultural and Forest Meteorology*, *182*, 277–291.

Richards, D. R., & Thompson, B. S. (2019). Urban ecosystems: A new frontier for payments for ecosystem services. *People and Nature*, *1*(2), 249–261.

Rossatto, D. R., Silva, L. d. C. R., Villalobos-Vega, R., Sternberg, L. D. S. L., & Franco, A. C. (2012). Depth of water uptake in woody plants relates to groundwater level and vegetation structure along a topographic gradient in a neotropical savanna. *Environmental and Experimental Botany*, *77*, 259–266.

Sawada, Y., & Koike, T. (2016). Ecosystem resilience to the millennium drought in southeast Australia (2001–2009). *Journal of Geophysical Research: Biogeosciences*, *121*, 2312–2327. https://doi.org/10.1002/2016JG003356

Saxton, K. E., & Rawls, W. J. (2006). Soil water characteristic estimates by texture and organic matter for hydrologic solutions. *Soil Science Society of America Journal*, *70*(5), 1569–1578.

Scott, R. L., Huxman, T. E., Williams, D. G., & Goodrich, D. C. (2006). Ecohydrological impacts of woody-plant encroachment: Seasonal patterns of water and carbon dioxide exchange within a semiarid riparian environment. *Global Change Biology*, *12*(2), 311–324.

Shields, C., & Tague, C. (2015). Ecohydrology in semiarid urban ecosystems: Modeling the relationship between connected impervious area and ecosystem productivity. *Water Resources Research*, *51*, 302–319. https://doi.org/10.1002/2014WR016108

Song, X. P., Tan, P. Y., Edwards, P., & Richards, D. (2018). The economic benefits and costs of trees in urban forest stewardship: A systematic review. *Urban Forestry & Urban Greening*, *29*, 162–170.

Soylu, M., Istanbulluoglu, E., Lenters, J., & Wang, T. (2011). Quantifying the impact of groundwater depth on evapotranspiration in a semi-arid grassland region. *Hydrology and Earth System Sciences*, *15*(3), 787–806.

Swann, A. L., Hoffman, F. M., Koven, C. D., & Randerson, J. T. (2016). Plant responses to increasing CO_2 reduce estimates of climate impacts on drought severity. *Proceedings of the National Academy of Sciences*, *113*(36), 10,019–10,024.

Tyrväinen, L., Pauleit, S., Seeland, K., & de Vries, S. (2005). Benefits and uses of urban forests and trees, *Urban forests and trees* (pp. 81–114): Springer.

van Dijk, A. I., Beck, H. E., Crosbie, R. S., de Jeu, R. A., Liu, Y. Y., Podger, G. M., et al. (2013). The Millennium Drought in southeast Australia (2001–2009): Natural and human causes and implications for water resources, ecosystems, economy, and society. *Water Resources Research*, *49*, 1040–1057. https://doi.org/10.1002/wrcr.20123

Van Genuchten, M. T. (1980). A closed-form equation for predicting the hydraulic conductivity of unsaturated soils 1. *Soil Science Society of America Journal*, *44*(5), 892–898.

Vincke, C., & Thiry, Y. (2008). Water table is a relevant source for water uptake by a scots pine (Pinus sylvestris L.) stand: Evidences from continuous evapotranspiration and water table monitoring. *Agricultural and Forest Meteorology*, *148*(10), 1419–1432.

Xiao, Q., McPherson, E., Simpson, J., & Ustin, S. (2007). Hydrologic processes at the urban residential scale. *Hydrological Processes: An International Journal*, *21*(16), 2174–2188.

Zencich, S. J., Froend, R. H., Turner, J. V., & Gailitis, V. (2002). Influence of groundwater depth on the seasonal sources of water accessed by Banksia tree species on a shallow, sandy coastal aquifer. *Oecologia*, *131*(1), 8–19.

Zipper, S. C., Schatz, J., Kucharik, C. J., & Loheide, S. P. (2017). Urban heat island-induced increases in evapotranspirative demand. *Geophysical Research Letters*, *44*, 873–881. https://doi.org/10.1002/2016GL072190

Zipper, S. C., Schatz, J., Singh, A., Kucharik, C. J., Townsend, P. A., & Loheide II, S. P. (2016). Urban heat island impacts on plant phenology: Intra-urban variability and response to land cover. *Environmental Research Letters*, *11*(5), 54023.